

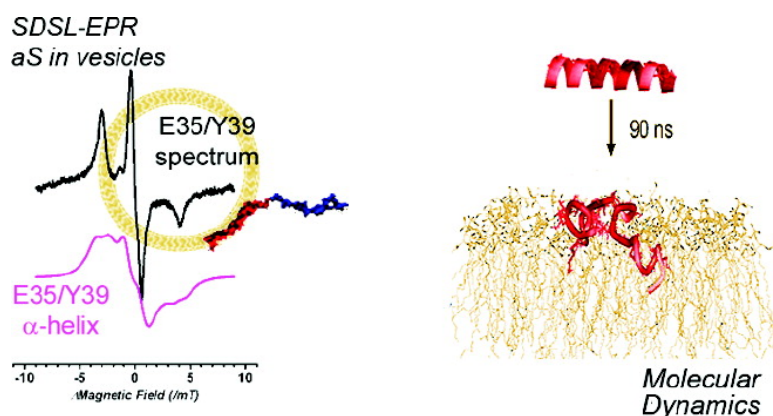
Communication

## Broken Helix in Vesicle and Micelle-Bound $\alpha$ -Synuclein: Insights from Site-Directed Spin Labeling-EPR Experiments and MD Simulations

Marco Bortolus, Fabio Tombolato, Isabella Tessari, Marco Bisaglia, Stefano Mammi, Luigi Bubacco, Alberta Ferrarini, and Anna Lisa Maniero

*J. Am. Chem. Soc.*, **2008**, 130 (21), 6690-6691 • DOI: 10.1021/ja8010429 • Publication Date (Web): 06 May 2008

Downloaded from <http://pubs.acs.org> on February 8, 2009



### More About This Article

Additional resources and features associated with this article are available within the HTML version:

- Supporting Information
- Links to the 1 articles that cite this article, as of the time of this article download
- Access to high resolution figures
- Links to articles and content related to this article
- Copyright permission to reproduce figures and/or text from this article

[View the Full Text HTML](#)

## Broken Helix in Vesicle and Micelle-Bound $\alpha$ -Synuclein: Insights from Site-Directed Spin Labeling-EPR Experiments and MD Simulations

Marco Bortolus,<sup>†</sup> Fabio Tombolato,<sup>†</sup> Isabella Tessari,<sup>‡</sup> Marco Bisaglia,<sup>‡</sup> Stefano Mammi,<sup>†</sup> Luigi Bubacco,<sup>‡</sup> Alberta Ferrarini,<sup>\*,†</sup> and Anna Lisa Maniero<sup>\*,†</sup>

*Dipartimento di Scienze Chimiche, Università di Padova, via Marzolo, 1, 35131 Padova, Italy and Dipartimento di Biologia, Università di Padova, viale Colombo 3, 35121 Padova, Italy*

Received February 13, 2008; E-mail: alberta.ferrarini@unipd.it; annalisa.maniero@unipd.it

Human  $\alpha$ -Synuclein (aS) is a 140 amino acid–protein strongly associated to both familial and sporadic cases of Parkinson’s disease.<sup>1</sup> The physiological role of aS is still elusive, although its nerve terminal localization<sup>2</sup> and its ability to interact with membranes seem to be the key factors for its physiological functions.

aS is a natively unfolded, soluble protein whose primary sequence is characterized by the presence of seven imperfect 11-residue repeats potentially able to fold into an amphipathic helix.<sup>3</sup> In the presence of sodium dodecyl sulfate (SDS) micelles or synthetic membranes, the first  $\sim$ 100 residues of aS undergo a conformational transition to a helical state.<sup>4</sup> The conformation of micelle-bound aS has been thoroughly investigated, and there is a general consensus on the presence of two helical portions, with a break in the 38–44 region.<sup>5–9</sup> On the contrary, the structure of aS bound to lipid vesicles, likely to be physiologically more relevant, is still a matter of debate. An uninterrupted helix has been proposed from site-directed spin labeling–electron paramagnetic resonance (SDSL-EPR) experiments in the presence of small unilamellar vesicles (SUV).<sup>10</sup> In that work, a systematic accessibility analysis in the 59–90 region was performed, whereas the helical arrangement for the 9–58 region was inferred from sparse data on selected mutants. We report here on an SDSL-EPR study of the controversial interhelix region of aS, when bound to either SUV or SDS micelles, accompanied by modeling of the spin label in the two proposed protein conformations. The investigation is completed by a Molecular Dynamics (MD) simulation of the 31–52 fragment interacting with a lipid bilayer. Our data show that the 38–44 region of aS exhibits a very similar behavior in micelles and in SUV. Specifically, we find evidence for a high degree of conformational disorder rather than for the formation of a continuous helical structure. CW-EPR experiments were performed on three double mutants of aS labeled with (1-oxy-2,2,5,5-tetramethylpyrroline-3-methyl)-methanethiosulfonate (MTSSL), that is, E35C/Y39C, Y39C/K43C, and E35C/K43C, in the presence of 1-palmitoyl-2-oleoyl-*sn*-glycero-3-[phospho-L-serine] (sodium salt) (POPS) SUV or SDS micelles. These mutants were chosen for the crucial location of the spin label in the region between the well-established helices of aS: the  $(i,i+4)$  and  $(i,i+8)$  sites, which correspond to periodicity typical of a helix, were specifically selected to probe the helical conformation. The distance analysis of the spectra was performed by the convolution method (see Supporting Information (SI)), assuming a Gaussian distribution.<sup>11,12</sup> The experimental data were compared to the interspin distance distributions obtained by modeling, taking into account the chain flexibility of MTSSL, for two selected conformations of aS, namely, an extended helix and the NMR structure of SDS-bound aS (PDB code 1XQ8). All

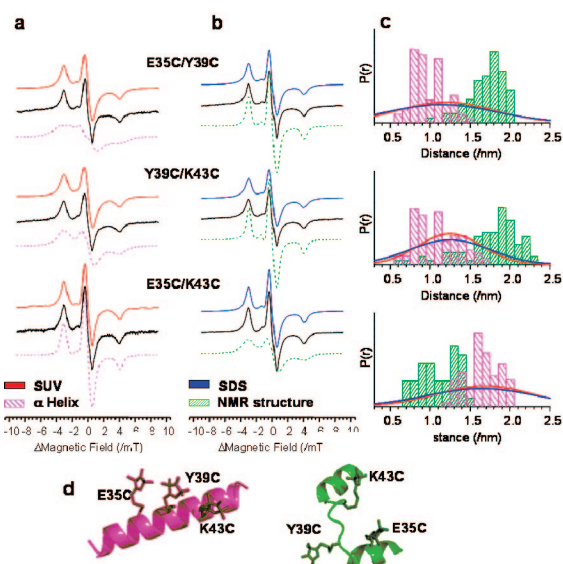


**Figure 1.** (a) Spectra of the double mutants in SUV (black), spectral fitting by the convolution method (red), spectra calculated using the distance distribution for MTSSL rotamers in an  $\alpha$ -helix (pink). (b) Spectra of the double mutants in SDS (black), spectral fitting (blue), spectra calculated for rotamers in the NMR structure (PDB code 1XQ8, green). (c) Gaussian distributions of distances obtained from fitting of the spectra in SUV (red) and in SDS (blue) and distance distribution calculated from the rotamers of MTSSL in the  $\alpha$ -helix (pink) and in the NMR structure (green). (d) Stick representation of the aS structures used for the rotamer calculations:  $\alpha$ -helix (pink) and NMR structure (green). Selected MTSSL rotamers are shown.

possible rotamers of the spin labels were generated, with the geometry determined in ref 13; only those rotamers were retained that are sterically allowed by the structure of the backbone and of the nearby side-chains. For the sake of comparison, EPR lineshapes of double mutants were then calculated, using the theoretical distance distributions (see SI). The experimental spectra of each double mutant are similar in SUV and SDS (Figure 1a,b), and as a consequence the derived distance distributions are almost identical (Figure 1c). This is in clear disagreement with the hypothesis of two different structures of the studied region of aS in SDS and SUV.<sup>10</sup> Our spectra are different from those reported in the literature for MTSSL linked to  $(i,i+4)$  and  $(i,i+8)$  sites of long  $\alpha$ -helices,<sup>11,14</sup> and our analysis leads to much wider distance distributions. Indeed, the main feature of all our experimental distributions is their broadness, clearly evident if compared with the distance distributions modeled either for the extended  $\alpha$ -helix or the NMR structure (Figure 1c, histograms). As a consequence, also the EPR lineshapes calculated using such distributions do not reproduce our experimental spectra. As far as SDS is concerned, the unsatisfactory comparison between experimental results and calculations based

<sup>†</sup> Dipartimento di Scienze Chimiche.

<sup>‡</sup> Dipartimento di Biologia.

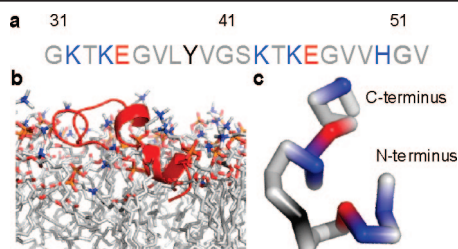


**Figure 2.** (a) Sequence of the aS fragment studied by MD; (b) snapshot of the fragment in POPC bilayer at the end of the MD trajectory (90 ns); and (c) tube representation of the backbone.

on the single NMR structure can be explained by the conformational disorder present in the 30–56 region.<sup>7,8</sup> The similarity of the results we have obtained in the two environments suggests that the observed distribution of backbone conformations for the linker region can be extended to SUV-bound aS. Some flexibility of the linker region, which allows it to fit to the environment while maintaining two antiparallel helices, is also consistent with possible changes in its local conformation as a function of the binding surface, which was hypothesized from pulsed EPR experiments in SDS and lyso-1-palmitoylphosphatidylglycerol (LPPG) micelles.<sup>9</sup>

The scarce propensity for a helical conformation of the 37–45 region upon lipid binding was confirmed by MD simulations. The 31–52 fragment of aS was studied in the presence of a 1-palmitoyl-2-oleoyl-*sn*-glycero-3-phosphocholine (POPC) bilayer (see SI); this peptide comprises two of the imperfect repeats that characterize the primary sequence of aS. In the starting configuration, the 31–52 fragment in an all  $\alpha$ -helical conformation was set in water, with its long axis parallel to the bilayer surface, at a distance of about 0.5 nm from the phosphates. The starting orientation maximizes the number of hydrophobic and hydrophilic residues facing the lipid bilayer and the water solution, respectively.<sup>6,7</sup> During the simulation, the fragment approaches the bilayer and starts to interact with the lipid headgroups through the C-terminal region. After 3 ns, the helix breaks in the proximity of Y39, and after that the unfolding process extends to the neighboring residues: a loop appears which evolves during the following about 10 ns, and the two helical ends move toward each other. From 20 to 90 ns of the trajectory the fragment penetrates into the bilayer, undergoing fluctuations about this partially unfolded structure, without dramatic transformations. A snapshot of the final configuration (90 ns) is shown in Figure 2. Interestingly, the central portion of the fragment can be viewed as a linker between the C- and N-terminal parts, which face each other in an antiparallel arrangement. The C terminal region, 43–52, retains helical character, whereas at the opposite end, between residues 31–37, helix fraying is observed. These results are in agreement with the structural characterization obtained by NMR in the presence of SDS micelles, as judged by the smaller C $^{\alpha}$  secondary shifts and lower order parameters for residues 30–37 compared with the other helical regions of aS.<sup>7</sup> The location of the C-terminal helical portion of the fragment, with its center 3–4 Å below the phosphates, compares well with the immersion depth of

the C-terminal helix estimated by EPR.<sup>10</sup> The behavior of the aS fragment is different from that observed in simulations of helical amphipathic peptides which, under analogous conditions, were found to remain roughly rod-shaped and predominantly helical when penetrating the bilayer.<sup>15</sup>

The main result of our investigation is that SUV-bound aS bears most of the features reported for it in micellar environment:<sup>5,7,8</sup> an unbroken helical structure of the region around residue 40 can be ruled out. Helix breaking does not appear to be a mere consequence of the constraints imposed by the small micellar dimensions,<sup>10</sup> but as an intrinsic feature of aS, when bound to amphipathic interfaces. Furthermore, we can confirm the picture of the interhelix region as characterized by conformational disorder, rather than exhibiting a single structure. This disorder might play a role in aS binding to synaptic vesicles, by allowing the protein to fit into amphipathic aggregates with different degrees of lipid packing strain.<sup>9</sup>

**Acknowledgment.** This work has been supported by Università degli Studi di Padova (PRAT 2005). Financial support by MUR is acknowledged by M.B., S.M., and L.B. (PRIN2005 and FIRB2004) and by A.F. and F.T. (PRIN2005). The convolution program was kindly provided by Prof. H. S. Mchaourab, Vanderbilt University, Nashville, TN. MD simulations were performed at the LICC facility (Università di Padova).

**Supporting Information Available:** Experimental details, additional EPR spectra, details on modeling and MD simulations. This material is available free of charge via the Internet at <http://pubs.acs.org>.

## References

- (1) Tofaris, G. K.; Spillantini, M. G. *Cell. Mol. Life Sci.* **2007**, *64*, 2194–2201.
- (2) Iwai, A.; Masliah, E.; Yoshimoto, M.; Ge, N.; Flanagan, L.; de Silva, H. A.; Kittel, A.; Saitoh, T. *Neuron* **1995**, *14*, 467–475.
- (3) Davidson, W. S.; Jonas, A.; Clayton, D. F.; George, J. M. *J. Biol. Chem.* **1998**, *273*, 9443–9449.
- (4) Eliezer, D.; Kutluay, E.; Bussell, R., Jr.; Browne, G. J. *Mol. Biol.* **2001**, *307*, 1061–1073.
- (5) Chandra, S.; Chen, X.; Rizo, J.; Jahn, R.; Sudhof, C. T. *J. Biol. Chem.* **2003**, *278*, 15313–15318.
- (6) Bussell, R.; Eliezer, D. *J. Mol. Biol.* **2003**, *329*, 763–778.
- (7) Ulmer, T. S.; Bax, A.; Cole, N. B.; Nussbaum, R. L. *J. Biol. Chem.* **2005**, *280*, 9595–9603.
- (8) Bisaglia, M.; Tessari, I.; Pinato, L.; Bellanda, M.; Giraudo, S.; Fasano, M.; Bergantino, E.; Bubacco, L.; Mammi, S. *Biochemistry* **2005**, *44*, 329–339.
- (9) Borbat, P.; Ramlall, T. F.; Freed, J. H.; Eliezer, D. *J. Am. Chem. Soc.* **2006**, *128*, 10004–10005.
- (10) Jao, C. C.; Der-Sarkissian, A.; Chen, J.; Langen, R. *Proc. Natl. Acad. Sci. U.S.A.* **2004**, *101*, 8331–8336.
- (11) Rabenstein, M. D.; Shin, Y.-K. *Proc. Natl. Acad. Sci. U.S.A.* **1995**, *92*, 8239–8243.
- (12) Alexander, N.; Al-Mestarihi, A.; Bortolus, M.; Mchaourab, H.; Meiler, J. *Structure* **2008**, *16*, 181–195.
- (13) Tombolato, F.; Ferrarini, A.; Freed, J. H. *J. Phys. Chem. B* **2006**, *110*, 26248–26259.
- (14) Altenbach, C.; Oh, K.-J.; Trabanino, R. J.; Hideg, K.; Hubbell, W. L. *Biochemistry* **2001**, *40*, 15471–15482.
- (15) (a) Shepherd, C. M.; Vogel, H. J.; Tieleman, D. P. *Biochem. J.* **2003**, *370*, 233–243. (b) Kandasamy, S. K.; Larson, R. G. *Chem. Phys. Lipids* **2004**, *132*, 113–132.

JA8010429